

Metal Complexes of *meso*-Amino-octaethylporphyrin and the Oxidation of Ni^{II}(*meso*-amino-octaethylporphyrin)

Natasza Sprutta, Sankar Prasad Rath, Marilyn M. Olmstead, and Alan L. Balch*

Department of Chemistry, University of California, Davis, California 95616

Received September 23, 2004

The crystal structures of *meso*-NH₂-OEPH₂, Ni^{II}(*meso*-NH₂-OEP), and Cu^{II}(*meso*-NH₂-OEP) (where OEP is the dianion of *meso*-amino-octaethylporphyrin) have been determined to examine the effects of the *meso*-substituent on the geometry of the ligand. Cu^{II}(*meso*-NH₂-OEP) has a nearly planar geometry while the free ligand itself and Ni^{II}(*meso*-NH₂-OEP) have *ruf* conformations. Ni^{II}(*meso*-NH₂-OEP) is much less reactive toward oxidation than are (py)₂Fe^{II}(*meso*-NH₂-OEP), ClFe^{III}(*meso*-NH₂-OEP), or Ni^{II}(*meso*-HO-OEP), which all undergo oxidation in pyridine solution when exposed to dioxygen. Treatment of Ni^{II}(*meso*-NH₂-OEP) with iron(III) chloride in chloroform solution does result in oxidation of the ligand in two separate processes. One involves oxygenation at the *trans*-*meso* position, while the other results in ring cleavage and removal of the amino function. The open-chain tetrapyrrole complex, Ni^{II}(OEB-CO₂Et), has been characterized by single-crystal X-ray diffraction and shown to contain a helical ligand with a four-coordinate nickel ion.

Introduction

Porphyrins are known for their stability toward oxidation. In particular iron porphyrins are used biologically to carry out numerous oxidations where highly oxidized forms participate without undergoing degradation.¹ Considerable effort has been expended to detect reactive iron porphyrins in highly oxidized states.^{2,3} In marked contrast, we recently reported that the iron(II) and iron(III) complexes of *meso*-amino-octaethylporphyrin (*meso*-NH₂-OEPH₂) undergo unusually rapid ring-opening when exposed to dioxygen in pyridine solution as shown in Scheme 1.^{4,5} In this process, the iron(II) complex, (py)₂Fe^{II}(*meso*-NH₂-OEP), reacts instantaneously with dioxygen to form a green intermediate that has been detected by UV-vis and ¹H NMR spectroscopy but has not yet been isolated or crystallized. Thus, the structures shown in Scheme 1 for this green intermediate,

while consistent with the spectroscopic data, are not fully established. Upon further exposure to dioxygen, this green intermediate is converted over a period of a day into the open-chain tetrapyrrole complex **A**, which has been isolated and crystallized. The open-chain tetrapyrrole **A** is also formed when a pyridine solution of ClFe^{III}(*meso*-NH₂-OEP) is treated with dioxygen. However, the green intermediate seen in the oxidation of the iron(II) complex, (py)₂Fe^{II}(*meso*-NH₂-OEP), is not detected in this reaction. The open-chain tetrapyrrole **A** undergoes further oxidation to form the tripyrrole complex, (py)₂Fe^{III}(HETP), and a second product, which has not yet been isolated or structurally characterized.

Here we examine some further aspects of the chemistry of *meso*-amino-octaethylporphyrin in order to examine the effect of the amino substituent on the structure of the macrocycle and on its reactivity. The environment of the *meso*-sites in hemes has been recognized to be sterically congested⁶ and substitution into the *meso*-positions can have significant structural effects. For example, Shelnut and co-workers have examined the effect of *meso*-nitro substitution in octaethylporphyrin on the conformation of the porphyrin macrocycle.⁷ We compare the structure of *meso*-NH₂-OEPH₂ with that of three of its metal complexes. Since nickel(II) porphyrin complexes are generally oxidation

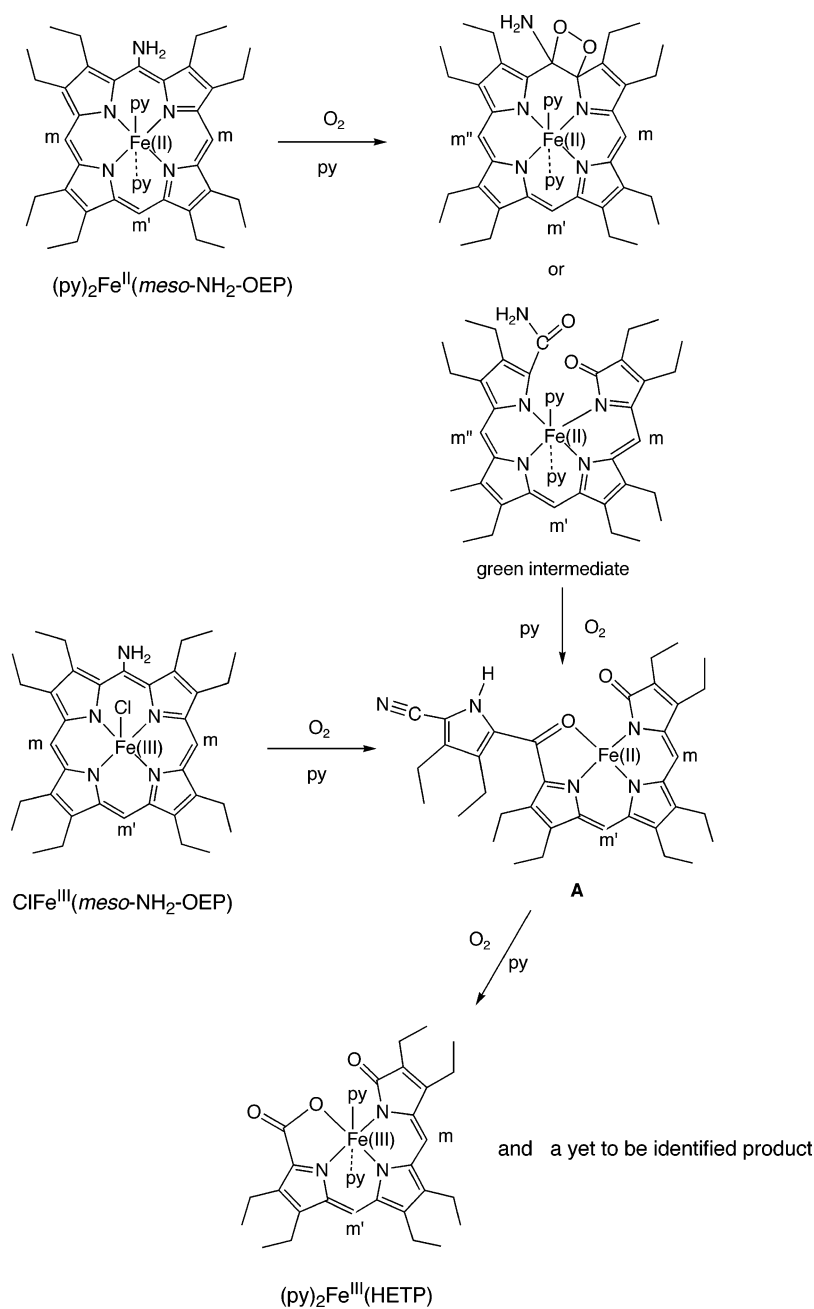
* To whom correspondence should be addressed. E-mail: albalch@ucdavis.edu.

- (1) Sono, M.; Roach, M. P.; Coulte, E. D.; Dawson, J. H. *Chem. Rev.* **1996**, *96*, 2841.
- (2) Chin, D. H.; La Mar, G. N.; Balch, A. L. *J. Am. Chem. Soc.* **1980**, *102*, 4344.
- (3) Groves, J. T.; Shalyeav, K.; Lee, J. In *The Porphyrin Handbook*; Kadish, K. M., Smith, K. M., Guillard, R., Eds.; Academic Press: New York, 2000; Vol. 4, p 17.
- (4) Kalish, H.; Lee, H. M.; Olmstead, M. M.; Latos-Grażyński, L.; Rath, S. P.; Balch, A. L. *J. Am. Chem. Soc.* **2003**, *125*, 4674.
- (5) Rath, S. P.; Kalish, H.; Latos-Grażyński, L.; Olmstead, M. M.; Balch, A. L. *J. Am. Chem. Soc.* **2004**, *126*, 646.

(6) Woodward, R. B. *Angew. Chem.* **1960**, *72*, 651.

(7) Anderson, K. K.; Hobbs, J. D.; Luo, L.; Stanley, K. D.; Quirke, J. M.; Shelnut, J. A. *J. Am. Chem. Soc.* **1993**, *115*, 12346.

Scheme 1



resistant, we have examined the oxidative stability of $Ni^{II}(meso-NH_2-OEP)$ and compared it to $ClFe^{III}(meso-NH_2-OEP)$, $(py)_2Fe^{II}(meso-NH_2-OEP)$, and $Ni^{II}(meso-HO-OEP)$. In pyridine solution, $Ni^{II}(meso-HO-OEP)$ is readily oxidized by dioxygen to form the air-stable radical, $(py)_2Ni^{II}(OEPO^{\bullet})$, which has been isolated and crystallized.⁸ While $(py)_2Ni^{II}(OEPO^{\bullet})$ is stable in the presence of pyridine, removal of pyridine results in the formation of the dimer, $Ni^{II}_2(OEPO)_2$, through C–C coupling at the *meso* carbon atoms.⁹

Results

The free base *meso*- NH_2 - $OEPH_2$ was prepared by the reduction of *meso*- NO_2 - $OEPH_2$ with tin and hydrochloric

acid by a previously reported route.¹⁰ Nickel(II) or copper(II) was inserted by a standard procedure to produce $Ni^{II}(meso-NH_2-OEP)$ or $Cu^{II}(meso-NH_2-OEP)$. Spectroscopic data for the products were consistent with those reported previously from different routes.¹¹

Crystallographic Characterization of *meso*- NH_2 - $OEPH_2$. The structure of the free base *meso*- NH_2 - $OEPH_2$ has been determined by X-ray crystallography. Crystal data are given in Table 1. Figure 1 shows a drawing of the molecule, which has no crystallographically imposed symmetry. Frequently the *meso* substituents in compounds derived from octaethylporphyrin display disorder in the position of that *meso* group in the solid state. Examples of

(8) Balch, A. L.; Noll, B. C.; Phillips, S. L.; Reid, S. M.; Zovinka, E. P. *Inorg. Chem.* **1993**, *32*, 4730.

(9) Balch, A. L.; Noll, B. C.; Reid, S. M.; Zovinka, E. P. *J. Am. Chem. Soc.* **1993**, *115*, 2531.

(10) Bonnett, R.; Stephenson, G. F. *J. Org. Chem.* **1965**, *30*, 2791.

(11) Crossley, M. J.; King, L. G.; Pyke, S. M.; Tansey, C. W. *J. Porphyrins Phthalocyanines* **2002**, *6*, 685.

Table 1. Crystallographic Data

	<i>meso</i> -NH ₂ -OEPH ₂	Ni ^{II} (<i>meso</i> -NH ₂ -OEP)	Cu ^{II} (<i>meso</i> -NH ₂ -OEP)	Ni ^{II} (OEB-CO ₂ Et)
formula	C ₃₆ H ₄₇ N ₅	C ₃₆ H ₄₅ N ₅ Ni	C ₃₆ H ₄₅ CuN ₅	C ₃₈ H ₄₈ N ₄ NiO ₃
fw	549.79	606.48	611.31	667.51
color/habit	black plate	red block	violet needle	black block
cryst syst	monoclinic	tetragonal	triclinic	monoclinic
space group	<i>P</i> 2 ₁ / <i>c</i>	<i>I</i> ₁ / <i>a</i>	<i>P</i> 1	<i>P</i> 2 ₁ / <i>n</i>
<i>a</i> , Å	20.321(9)	14.7645(12)	4.7346(9)	17.447(6)
<i>b</i> , Å	15.106(7)	14.7645(12)	13.096(3)	14.066(5)
<i>c</i> , Å	9.863(5)	13.9225(14)	13.422(3)	29.452(10)
α, deg	90	90	65.95(3)	90
β, deg	94.243(9)	90	89.64(3)	105.648(6)
γ, deg	90	90	86.76(3)	90
<i>V</i> , Å ³	3020(2)	3035.0(5)	758.6(3)	6960(4)
<i>Z</i>	4	4	1	8
<i>T</i> , °C	90(2)	130(2)	130(2)	90(2)
λ, Å	0.71073	1.54178	1.54178	0.71073
ρ, g/cm ³	1.209	1.327	1.338	1.274
μ, mm ⁻¹	0.072	1.172	1.266	0.599
R1 ^a (obsd data)	0.0813	0.031	0.039	0.066
wR2 ^a (all data, F ² refinement)	0.207	0.078	0.101	0.181

a

$$R1 = \frac{\sum ||F_o| - |F_c||}{\sum |F_o|}; wR2 = \sqrt{\frac{\sum [w(F_o^2 - F_c^2)^2]}{\sum [w(F_o^2)^2]}}$$

such cases where significant disorder is present include ClFe^{III}(*meso*-NC-OEP),¹² (py)₂Fe(OEPO),¹³ and Zn^{II}(OE-PO*).¹⁴ However, in *meso*-NH₂-OEPH₂ the amino group is ordered. The N-H groups lie on one side of the porphyrin, while the adjacent ethyl groups point toward the opposite side. The internal N-H groups are also ordered and located on opposite pyrrole rings as is the case in OEPH₂.¹⁵ Each N-H group of the amino substituent on one porphyrin forms a hydrogen bond to an inner nitrogen atom of an adjacent molecule. As part C of Figure 1 shows, these hydrogen bonding interactions between molecules connect the molecules together in continuous chains.

The porphyrin ring in *meso*-NH₂-OEPH₂ is somewhat distorted from planarity. Figure 2 shows a comparison of the out-of-plane displacements (in units of 0.01 Å) of the core atoms of *meso*-NH₂-OEPH₂ with several other relevant porphyrins. The out-of-plane displacements for *meso*-NH₂-OEPH₂ are remarkably similar to those observed previously for ClFe^{III}(*meso*-NH₂-OEP). Such distortions of porphyrins from planarity follow the low-frequency, normal vibrational modes of the porphyrin macrocycle and can involve deformations that have been designated as *sad*, *ruf*, *dom*, *wav*(*x*), *wav*(*y*) and *pro*.^{16,17} In *meso*-NH₂-OEPH₂ and ClFe^{III}(*meso*-NH₂-OEP) the porphyrin cores assume a *ruf* conformation, and in both cases there are important hydrogen bonding

interactions between the molecules. In ClFe^{III}(*meso*-NH₂-OEP) hydrogen bonding occurs between the amino group of one molecule and the axial chloride ligand of a neighboring molecule.

Crystallographic Characterization of Ni^{II}(*meso*-NH₂-OEP). The crystallographically determined structure of Ni^{II}(*meso*-NH₂-OEP) is shown in Figure 3. The complex crystallizes in the tetragonal space group *I*₁/*a* with the nickel atom residing at a site of *S*₄ (4) symmetry. Consequently, the amino group is disordered over four equivalent sites with 0.25 occupancy at each. For clarity, only one of these sites is shown in Figure 3. Unlike the situation in *meso*-NH₂-OEPH₂ and in ClFe^{III}(*meso*-NH₂-OEP), the amino group in Ni^{II}(*meso*-NH₂-OEP) does not engage in hydrogen bonding. As Figure 3 shows, the coordination about the nickel ion is planar but the porphyrin itself is significantly distorted from planarity.

The structure of Ni^{II}(*meso*-NH₂-OEP) is readily compared to those of Ni^{II}(OEP) and Ni^{II}(*meso*-HO-OEP). Ni^{II}(OEP) crystallizes in three polymorphic forms: a triclinic A form,¹⁸ a second triclinic B form,¹⁹ and a tetragonal form.²⁰ Each contains four-coordinate, planar nickel, but in the tetragonal form the Ni-N bond length is compressed to only 1.929 Å. As a result the porphyrin is distorted from planarity as the data in Figure 2 show. The Ni-N distance in Ni^{II}(*meso*-NH₂-OEP) is similarly short, 1.9164(16) Å. Ni^{II}(*meso*-HO-OEP) also crystallizes in the tetragonal space group *I*₁/*a*, and again the *meso*-HO group is disordered over four equivalent sites.⁸ The Ni-N distance in Ni^{II}(*meso*-HO-OEP) is also short, 1.915(6) Å. Notice that the out-of-plane displacements

(12) Kalish, H.; Camp, J. E.; Stepien, M.; Latos-Grażyński, L.; Olmstead, M. M.; Balch, A. L. *Inorg. Chem.* **2002**, *41*, 989.(13) Balch, A. L.; Koerner, R.; Latos-Grażyński, L.; Noll, B. C. *J. Am. Chem. Soc.* **1996**, *118*, 2760.(14) Balch, A. L.; Noll, B. C.; Zovinka, E. P. *J. Am. Chem. Soc.* **1991**, *114*, 3380.(15) Lauher, J. W.; Ibers, J. A. *J. Am. Chem. Soc.* **1973**, *95*, 5148.(16) Jentzen, W.; Song, X.-Z.; Shelnut, J. A. *J. Phys. Chem. B* **1997**, *101*, 1684.(17) Shelnut, J. A.; Song, X.-Z.; Ma, J.-G.; Jia, S.-L.; Jentzen, W.; Medforth, C. J. *Chem. Soc. Rev.* **1998**, *27*, 31.(18) Cullen, D. L.; Meyer, E. F., Jr. *J. Am. Chem. Soc.* **1974**, *96*, 2095.(19) Brennan, T. D.; Scheidt, W. R.; Shelnut, J. A. *J. Am. Chem. Soc.* **1988**, *110*, 3919.(20) Meyer, E. F., Jr. *Acta Crystallogr.* **1972**, *B28*, 2162.

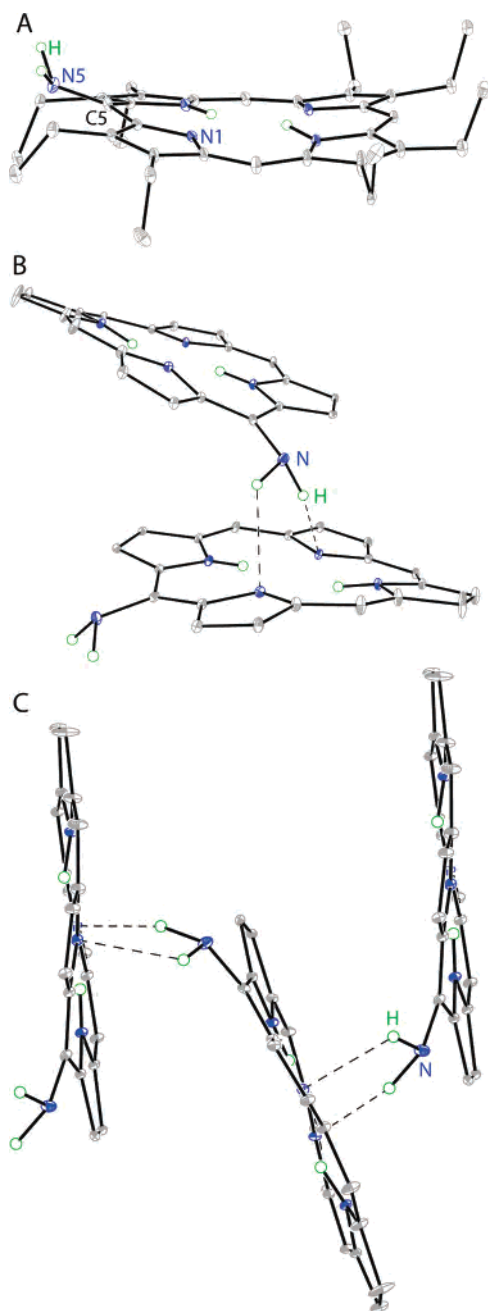


Figure 1. Three perspective views of *meso*-NH₂-OEPH₂ showing 30% thermal contours. Part A shows the asymmetric unit, part B shows the hydrogen bonding interactions between the amino group of one molecule and the pyrrole nitrogen atoms of another molecule, while part C shows the hydrogen bonding between three molecules. The nitrogen atoms are blue, the hydrogen atoms of the amino group (which for clarity are the only hydrogen atoms shown) are green, and the carbon atoms are gray. In B and C, the ethyl groups are removed for clarity.

of the porphyrin core atoms in Ni^{II}(*meso*-NH₂-OEP), in the tetragonal polymorph of Ni^{II}(OEP), and in Ni^{II}(*meso*-HO-OEP) are similar as seen in Figure 3.

Crystallographic Characterization of Cu^{II}(*meso*-NH₂-OEP). Figure 4 shows two views of Cu^{II}(*meso*-NH₂-OEP). The complex crystallizes in the triclinic space group *P* $\bar{1}$ with the copper atom located on a center of symmetry. The asymmetric unit consists of half of the molecule. The amino group is disordered over two sites. For clarity only one of these is shown in Figure 4. The other amino group lies on

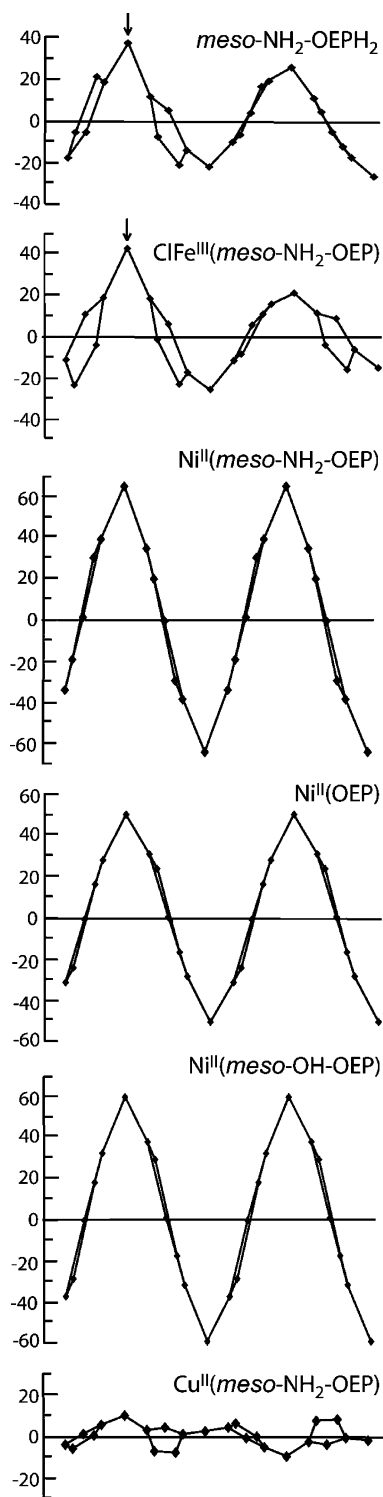


Figure 2. Diagrams comparing the out-of-plane displacements (in units of 0.01 Å) for the porphyrin core atoms from the mean plane of the porphyrin for *meso*-NH₂-OEPH₂, ClFe^{III}(*meso*-NH₂-OEP),⁵ Ni^{II}(*meso*-NH₂-OEP), Ni^{II}(OEP) (tetragonal polymorph),²⁰ Ni^{II}(*meso*-HO-OEP),⁸ and Cu^{II}(*meso*-NH₂-OEP). The *meso*-substituents are attached to the carbon atoms denoted by arrows.

the opposite *meso* site as required by the center of symmetry. The copper ion has planar geometry and Cu–N distances, 2.017(2) and 2.012(3) Å, that are significantly longer than the Ni–N distance (1.9164(16) Å) in Ni^{II}(*meso*-NH₂-OEP). As seen from the data in Figure 2, the porphyrin in Cu^{II}(*meso*-NH₂-OEP) is more nearly planar than it is in *meso*-

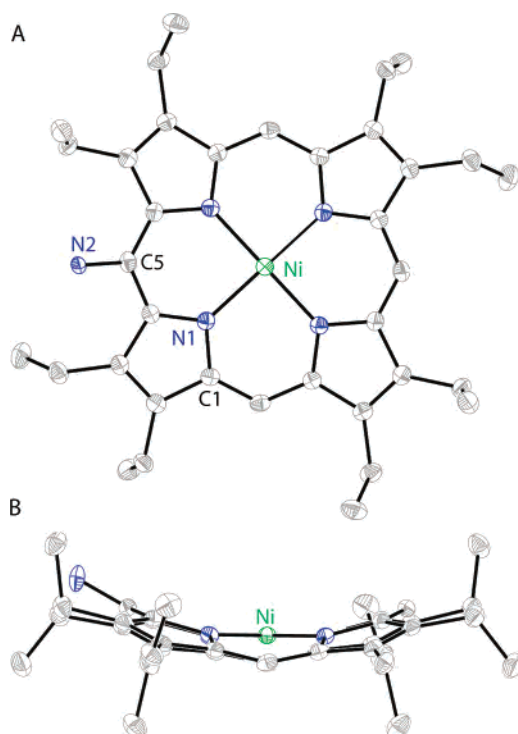


Figure 3. Two views of $\text{Ni}^{\text{II}}(\text{meso-NH}_2\text{-OEP})$ with 30% thermal contours. The amino group is disordered, and only one site with 0.25 occupancy is shown in the drawing. The amino group also resides at each of the other three meso positions with 0.25 occupancy.

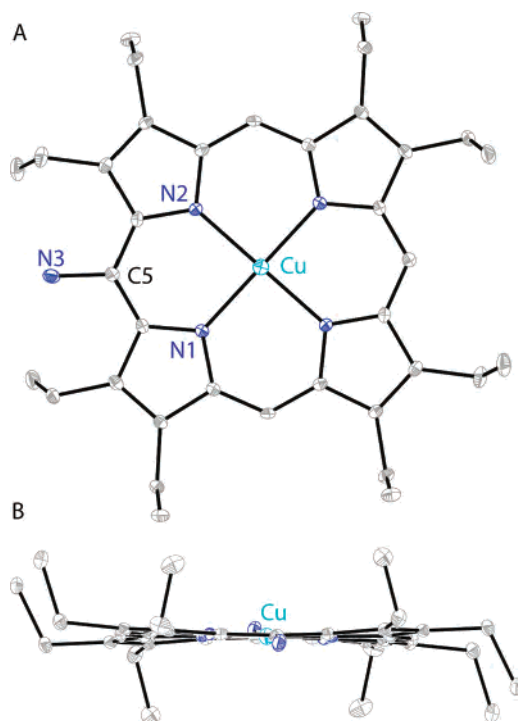


Figure 4. Two views of $\text{Cu}^{\text{II}}(\text{meso-NH}_2\text{-OEP})$ with 30% thermal contours. Only one site with 0.5 occupancy for the disordered amino group is shown. The amino group also is present at the site opposite the one shown, again with 0.5 occupancy.

$\text{NH}_2\text{-OEPH}_2$, $\text{ClFe}^{\text{III}}(\text{meso-NH}_2\text{-OEP})$, or $\text{Ni}^{\text{II}}(\text{meso-NH}_2\text{-OEP})$. For comparison $\text{Cu}^{\text{II}}(\text{OEP})$ has a Cu-N distance of 1.999(3) and 1.996(3) Å.²¹

(21) Pak, R.; Scheidt, W. R. *Acta Crystallogr., Sect. C* **1991**, *C47*, 431.

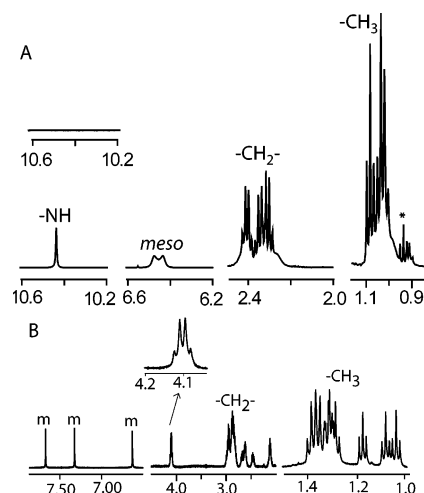
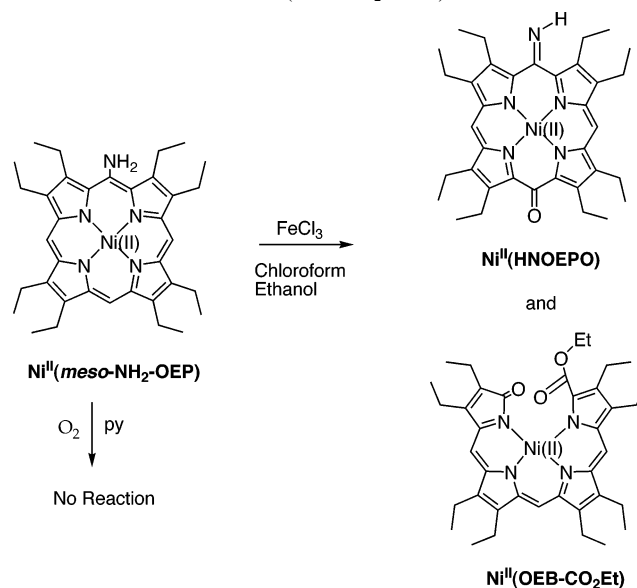


Figure 5. 500 MHz ^1H NMR spectra of (A) $\text{Ni}^{\text{II}}(\text{HNOEPO})$ and (B) $\text{Ni}^{\text{II}}(\text{OEB-CO}_2\text{Et})$ in chloroform- d solution. The insert to part A shows a portion of the spectrum after the sample was shaken with D_2O .

Scheme 2. Oxidation of $\text{Ni}^{\text{II}}(\text{meso-NH}_2\text{-OEP})$

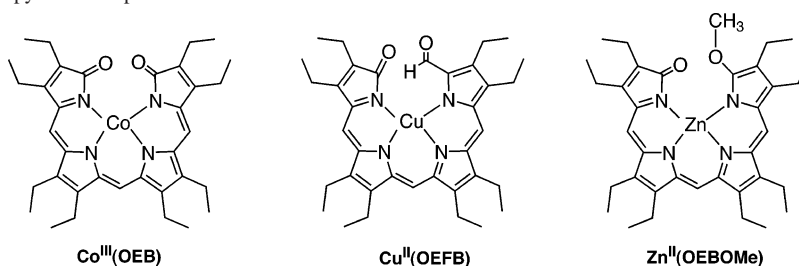


Oxidation of $\text{Ni}^{\text{II}}(\text{meso-NH}_2\text{-OEP})$. Unlike the case with $(\text{py})_2\text{Fe}^{\text{II}}(\text{meso-NH}_2\text{-OEP})$, $\text{ClFe}^{\text{III}}(\text{meso-NH}_2\text{-OEP})$, or $\text{Ni}^{\text{II}}(\text{meso-HO-OEP})$, solutions of $\text{Ni}^{\text{II}}(\text{meso-NH}_2\text{-OEP})$ in pyridine are stable to exposure to dioxygen.²² Consequently, we examined the reactivity of $\text{Ni}^{\text{II}}(\text{meso-NH}_2\text{-OEP})$ with other oxidants. Treatment of $\text{Ni}^{\text{II}}(\text{meso-NH}_2\text{-OEP})$ with iron(III) chloride in ethanol-stabilized chloroform results in a slow oxidation. As shown in Scheme 2, two products have been isolated from this reaction.

The major product is $\text{Ni}^{\text{II}}(\text{HNOEPO})$, which has been isolated as violet crystals in 44% yield. The ^1H NMR spectrum of the complex is shown in part A of Figure 5. Key features of the spectrum are the presence of a resonance at 10.44 ppm due to the N-H group and two meso resonances of equal intensity, which result from the positioning of the N-H group. The N-H group is constrained to lie in the plane of the macrocycle. Consequently, that proton

(22) Under these conditions, $\text{Cu}^{\text{II}}(\text{meso-NH}_2\text{-OEP})$ reacts with dioxygen, but we have been unable to isolate any of the oxidation products.

Chart 1. Helical Linear Tetrapyrrole Complexes



is closer to one meso C–H group than to the other. To obtain this spectrum, the sample was treated with solid potassium hydroxide to remove acid impurities. Small amounts of acid cause exchange of the N–H proton and result in coalescence of the two meso proton resonances. The N–H proton resonance is lost when a sample of Ni^{II}(HNOEPO) is treated with D₂O. Crystals of the complex suitable for X-ray crystallography have been obtained. These form in the tetragonal space group *I*₁/*a*. Consequently, they are isostructural with Ni^{II}(*meso*-NH₂-OEP), the tetragonal form of Ni^{II}(OEP),²⁰ and Ni^{II}(OEPO₂).²³ In this situation, the meso substituents are disordered over four equivalent sites, which obviates the ability to distinguish between the N–H and O substituents.

The second product resulting from the oxidation of Ni^{II}(*meso*-NH₂-OEP) is the ring opened tetrapyrrole complex, Ni^{II}(OEB–CO₂Et), which has been isolated in 10% yield. The added ethyl group in the ester portion of the complex arises from ethanol, which is present as a stabilizer in the solvent, chloroform. Several metal complexes of other ring-opened tetrapyrroles have been characterized including Co^{III}(OEB),²⁴ Cu^{II}(OEFB),²⁵ and Zn^{II}(OEB–OMe)²⁶ whose structures are shown in Chart 1.

The ¹H NMR spectrum of Ni^{II}(OEB–CO₂Et) is shown in part B of Figure 5. The spectrum shows three meso resonances of equal intensity at 7.64, 7.30, and 6.60 ppm and a unique methylene quartet at 4.10 ppm due to the ester group as well as other methylene resonances in the 3–2 ppm range and methyl resonances in the 1.4 to 1.0 ppm region. The UV–vis spectrum shows bands at 304, 322, 418 (Soret), and 796 nm. The feature at 796 nm is indicative of the presence of a ring-opened tetrapyrrole. For comparison the UV–vis spectrum of Ni^{II}(OEFB) has λ_{max} at 308, 424, and 802 nm.²⁵

Crystallographic Characterization of Ni^{II}(OEB–CO₂Et).

The complex crystallizes with two independent molecules in the asymmetric unit. The structure of one of these is shown in Figure 6. The other one is similar. Selected bond distances and angles are given in the caption to Figure 6.

Ni^{II}(OEB–CO₂Et) has a helical structure that is similar to those of the crystallographically characterized complexes,

Co^{III}(OEB),²⁴ Ni^{II}(OEFB),²⁵ and Zn^{II}(OEB–OMe).²⁶ The overlap of the terminal portions of the tetrapyrrole ligand prohibit the ligand and the metal ion from assuming a completely planar geometry. The nickel ion has a four-coordinate geometry with Ni–N distances that span a narrow range, 1.864(3) to 1.884(3) Å. These distances are shorter than the corresponding distance, 1.9164(16) Å, in Ni^{II}(*meso*-NH₂-OEP). The open-chain tetrapyrrole is simply more flexible and can more readily adjust to accommodate the metal ion it surrounds. The helical nature of the ligand distorts the geometry of the nickel ion so that it is not planar. While the *cis*-N–Ni–N angles cluster in a narrow range (90.37(12)° to 93.35(12)°) about 90°, the *trans*-N–Ni–N angles (161.02(12)° and 161.03(12)°) deviate significantly from linearity. There is a center of symmetry in the space

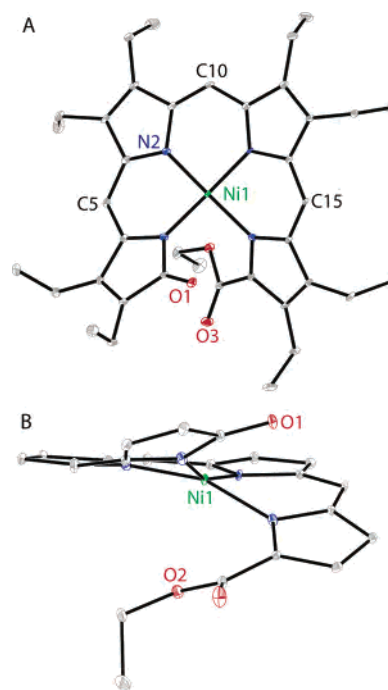


Figure 6. Two views of Ni^{II}(OEB–CO₂Et) with 30% thermal contours. For clarity the ethyl groups were omitted in part B. Selected bond distances (Å): molecule 1, Ni(1)–N(1), 1.864(3); Ni(1)–N(2), 1.884(3); Ni(1)–N(3), 1.875(3); Ni(1)–N(4), 1.876(3); O(1)–C(1), 1.217(4); O(2)–C(20), 1.353(4); O(2)–C(37), 1.450(4); O(3)–C(20), 1.203(4); molecule 2, Ni(51)–N(51), 1.879(3); Ni(51)–N(52), 1.887(3); Ni(51)–N(53), 1.876(3); Ni(51)–N(54), 1.878(3); O(51)–C(51), 1.216(4); O(52)–C(70), 1.361(4); O(52)–C(87), 1.449(4); O(53)–C(70), 1.207(4). Selected bond angles (deg): molecule 1, N(1)–Ni(1)–N(2), 91.26(12); N(1)–Ni(1)–N(3), 161.02(12); N(1)–Ni(1)–N(4), 91.22(12); N(3)–Ni(1)–N(4), 90.37(12); N(3)–Ni(1)–N(2), 93.35(12); N(4)–Ni(1)–N(2), 161.03(12); molecule 2, N(51)–Ni(51)–N(52), 91.33(12); N(53)–Ni(51)–N(54), 90.62(12); N(53)–Ni(51)–N(51), 161.07(12); N(54)–Ni(51)–N(51), 91.20(12); N(53)–Ni(51)–N(52), 93.29(12); N(54)–Ni(51)–N(52), 160.29(12).

(23) Balch, A. L.; Olmstead, M. M.; Phillips, S. L. *Inorg. Chem.* **1993**, *32*, 3931.

(24) Balch, A. L.; Mazzanti, M.; Noll, B. C.; Olmstead, M. M. *J. Am. Chem. Soc.* **1994**, *116*, 9114.

(25) Koerner, R.; Olmstead, M. M.; Ozarowski, A.; Phillips, S. L.; Van Calcar, P. M.; Winkler, K.; Balch, A. L. *J. Am. Chem. Soc.* **1998**, *120*, 1274.

(26) Latos-Grażyński, L.; Johnson, J.; Attar, S.; Olmstead, M. M.; Balch, A. L. *Inorg. Chem.* **1998**, *37*, 4493.

group $P2_1/n$, so the crystal of $\text{Ni}^{\text{II}}(\text{OEB}-\text{CO}_2\text{Et})$ contains a racemate of the two enantiomeric helices.

Discussion

The results reported here demonstrate that *meso*- NH_2 -OEPH₂ and its complexes can assume a variety of structures with varying degrees of planarity and that the amino group itself does not impose a particular geometry on the macrocycle. Thus, $\text{Cu}^{\text{II}}(\text{meso-NH}_2\text{-OEP})$ assumes a nearly planar geometry as seen in Figure 2, while $\text{Ni}^{\text{II}}(\text{meso-NH}_2\text{-OEP})$, which also contains a planar, four-coordinate metal ion, adopts a *ruf* conformation. The position of the amino group is ordered in the free ligand, *meso*- NH_2 -OEPH₂ and in $\text{ClFe}^{\text{III}}(\text{meso-NH}_2\text{-OEP})$ where specific hydrogen bonding interactions between molecules are present. In $\text{Ni}^{\text{II}}(\text{meso-NH}_2\text{-OEP})$ and $\text{Cu}^{\text{II}}(\text{meso-NH}_2\text{-OEP})$, however, the structural features that allowed hydrogen bonding, the uncoordinated inner nitrogen atoms of the porphyrin or the axial chloride ligand, are absent and the amino group is disordered in the crystals.

$\text{Ni}^{\text{II}}(\text{meso-NH}_2\text{-OEP})$ is considerably more robust toward oxidation than are the complexes, $\text{ClFe}^{\text{III}}(\text{meso-NH}_2\text{-OEP})$, $(\text{py})_2\text{Fe}^{\text{II}}(\text{meso-NH}_2\text{-OEP})$, or $\text{Ni}^{\text{II}}(\text{meso-HO-OEP})$. In particular pyridine solutions of $\text{Ni}^{\text{II}}(\text{meso-NH}_2\text{-OEP})$ do not react with dioxygen. Clearly, the simple presence of *meso*-amino-octaethylporphyrin as a ligand does not produce complexes that are necessarily susceptible to oxidation. However, iron(III) chloride does oxidize $\text{Ni}^{\text{II}}(\text{meso-NH}_2\text{-OEP})$ as shown in Scheme 2. Two rather different products, $\text{Ni}^{\text{II}}(\text{HNOEPO})$ and $\text{Ni}^{\text{III}}(\text{OEB}-\text{CO}_2\text{Et})$, form. Since their structures are so different, two parallel paths for oxidation are involved. In one, the *meso* carbon trans to the amino function is attacked and oxygenated. A similar oxidation of $\text{Zn}^{\text{II}}(\text{meso-NH}_2\text{-OEP})$ to form $\text{Zn}^{\text{II}}(\text{HNOEPO})$ has been briefly reported.²⁷ In the other reaction, the porphyrin undergoes ring-opening at the site of the amino group which is no longer present in the product, $\text{Ni}^{\text{II}}(\text{OEB}-\text{CO}_2\text{Et})$. This latter reaction results in the same sort of ring opening of the porphyrin as occurs when $(\text{py})_2\text{Fe}^{\text{II}}(\text{meso-NH}_2\text{-OEP})$ or $\text{ClFe}^{\text{III}}(\text{meso-NH}_2\text{-OEP})$ are exposed to dioxygen in pyridine solution.

Experimental Section

Materials. Octaethylporphyrin was purchased from Mid Century. *meso*- NH_2 -OEPH₂ was prepared by stannous chloride reduction of *meso*- NO_2 -OEPH₂ as described previously and crystallized from chloroform/methanol.¹¹ All solvents were used as purchased except pyridine-*d*₅ which was used after distillation from KOH.

$\text{Ni}^{\text{II}}(\text{meso-NH}_2\text{-OEP})$. A 50 mg (0.091 mmol) portion of 5-amino-octaethylporphyrin was dissolved in 100 mL of chloroform. A 5 mL portion of a saturated solution of nickel(II) acetate in methanol was added. The resulting solution was heated under reflux for 20 min. The solution was evaporated to dryness, and the resulting solid was dissolved in 50 mL of dichloromethane. This dichloromethane solution was washed with water and evaporated. Column chromatography on basic alumina using dichloromethane as an eluent gave a $\text{Ni}^{\text{II}}(\text{meso-NH}_2\text{-OEP})$ as the first, red band to

elute from the column; yield 52.1 mg (95%). Crystals were grown by diffusion of methanol into a chloroform solution of the complex. The product was identified by comparison of its ¹H NMR and UV-vis spectra with those obtained previously.¹¹

$\text{Cu}^{\text{II}}(\text{meso-NH}_2\text{-OEP})$. A 3 mL portion of a saturated solution of copper acetate in methanol was added to a solution of 50 mg (0.091 mmol) of *meso*- NH_2 -OEPH₂ in 50 mL of chloroform. After stirring for 10 min, the mixture was evaporated to dryness. The solid residue was dissolved in 50 mL of dichloromethane, filtered, and washed with water. The organic layer was separated and evaporated. Column chromatography on basic alumina using dichloromethane as an eluent gave a red band containing $\text{Cu}^{\text{II}}(\text{meso-NH}_2\text{-OEP})$ as a first fraction. This band was collected and evaporated to give solid $\text{Cu}^{\text{II}}(\text{meso-NH}_2\text{-OEP})$; yield 54.5 mg (98%). Spectroscopic data for the product were consistent with those reported earlier.¹¹ Crystals were grown by diffusion of methanol into a chloroform solution of $\text{Cu}^{\text{II}}(\text{meso-NH}_2\text{-OEP})$.

Oxidation of $\text{Ni}^{\text{II}}(\text{meso-NH}_2\text{-OEP})$ with Ferric Chloride: Formation of $\text{Ni}^{\text{II}}(\text{OEPONH})$ and $\text{Ni}^{\text{II}}(\text{OEB}-\text{CO}_2\text{Et})$. A 38 mg (0.063 mmol) sample of $\text{Ni}^{\text{II}}(\text{meso-NH}_2\text{-OEP})$ and a 100 mg (0.617 mmol) portion of iron(III) chloride were dissolved in 200 mL of chloroform. The resulting mixture was stirred for 18 h. The solution was evaporated to dryness. The solid that formed was dissolved in dichloromethane and chromatographed on basic alumina. The first fraction (red) contained unreacted $\text{Ni}^{\text{II}}(\text{meso-NH}_2\text{-OEP})$. The second (yellow-brownish) fraction was subsequently identified as containing $\text{Ni}^{\text{II}}(\text{HNOEPO})$. The third fraction was eluted with a mixture of chloroform:methanol (80:20, v/v). This yellow-green solution was found to contain $\text{Ni}^{\text{II}}(\text{OEB}-\text{CO}_2\text{Et})$ and two other unidentified compounds.

A second round of chromatography for the second yellow-brown fraction on silica gel (60–200 mesh) with dichloromethane as an eluent gave pure $\text{Ni}^{\text{II}}(\text{HNOEPO})$. Recrystallization of this sample from chloroform/methanol gave violet crystals of $\text{Ni}^{\text{II}}(\text{HNOEPO})$: yield 16.7 mg (44%). UV-vis spectrum in chloroform: λ_{max} [nm] (log ϵ) 326 (4.39), 456 (4.74), 536 (4.04), 660 (br). 500 MHz ¹H NMR spectrum (chloroform-*d*): δ [ppm] = 10.44 (NH, 1H, s), 6.46 (*meso*, 2H, s), 2.25–2.45 (methylene, 16H, m), 0.95–1.12 (methyl, 24H, m). Mass spectrum (MALDI) found: $[\text{M} + 1] m/z = 620.3092$, C₃₆H₄₄N₅ONi. $\text{Ni}^{\text{II}}(\text{HNOEPO})$ crystallized from chloroform/methanol in the tetragonal space group I_1/a with $a = 14.698(3)$ Å and $c = 14.200(6)$ Å.

$\text{Ni}^{\text{II}}(\text{OEB}-\text{CO}_2\text{Et})$ was purified by recrystallization from chloroform yield, 4 mg (10%). Crystals were grown by slow evaporation of a chloroform solution of the complex. UV-vis spectrum in dichloromethane: λ_{max} , [nm] (log ϵ) 304(4.40), 322(4.32), 418-(4.40), 796(4.00). 500 MHz ¹H NMR (dichloromethane-*d*₂): δ [ppm] = 7.64 (*meso*, 1H, s), 7.30 (*meso*, 1H, s), 6.60 (*meso*, 1H, s), 4.10 (methylene, 2H, q), 3.00–2.761 (methylene, 8H, m), 2.67 (methylene, 1H, q), 2.46 (methylene, 1H, q), 2.60 (methylene, 2H, q), 2.12 (methylene, 2H, q), 1.39–1.22 (methyl, 15H, m), 1.15 (methyl, 3H, t), 1.06 (methyl, 3H, t), 1.01 (methyl, 3H, t).

X-ray Data Collection. Crystals were coated with a light hydrocarbon oil and mounted in the 90 K dinitrogen stream of a Bruker SMART 1000 diffractometer equipped with CRYO Industries low-temperature apparatus for *meso*- NH_2 -OEPH₂ and for $\text{Ni}^{\text{II}}(\text{OEB}-\text{CO}_2\text{Et})$ or in the 130(2) K dinitrogen stream of a Siemens P4 diffractometer and a Cu rotating anode that was equipped with Siemens LT-2 low-temperature apparatus for $\text{Ni}^{\text{II}}(\text{meso-NH}_2\text{-OEP})$ and $\text{Cu}^{\text{II}}(\text{meso-NH}_2\text{-OEP})$. Crystal data are given in Table 1.

Solution and Structure Refinement. Scattering factors and correction for anomalous dispersion were taken from a standard

(27) Fuhrhop, J.-H. *J. Chem. Soc., Chem. Commun.* **1970**, 781.

source.²⁸ An absorption correction was applied.²⁹ The solution of the structure was obtained by direct methods with SHELXS-97 and subsequent cycles of least-squares refinement on F^2 with SHELXL-97.

Instrumentation. ^1H NMR spectra were recorded on a Bruker Avance 500 FT spectrometer (the ^1H frequency is 500.13 MHz).

- (28) *International Tables for Crystallography*; Kluwer Academic Publishers: Dordrecht, The Netherlands, 1992.
- (29) (a) For *meso*- NH_2 -OEPH₂ and $\text{Ni}^{\text{II}}(\text{OEB}-\text{CO}_2\text{Et})$: Sheldrick, G. M. *SADABS 2.10*; University of Göttingen: Göttingen, Germany, 2003. (b) For $\text{Ni}^{\text{II}}(\text{meso-NH}_2\text{-OEP})$ and $\text{Cu}^{\text{II}}(\text{meso-NH}_2\text{-OEP})$: Parkin, S.; Moessi, B.; Hope, H. *XABS2. J. Appl. Crystallogr.* **1995**, 28, 53.

Acknowledgment. We thank the NIH (Grant GM-26226 to A.L.B.) for financial support and the NSF (Grant OSTI 97-24412) for partial funding of the 500 MHz NMR spectrometer.

Supporting Information Available: X-ray crystallographic files in CIF format for *meso*- NH_2 -OEPH₂, $\text{Ni}^{\text{II}}(\text{meso-NH}_2\text{-OEP})$, $\text{Cu}^{\text{II}}(\text{meso-NH}_2\text{-OEP})$, and $\text{Ni}^{\text{II}}(\text{OEB}-\text{CO}_2\text{Et})$. This material is available free of charge via the Internet at <http://pubs.acs.org>.

IC0486623